Abridged version

KAWASAKI STEEL TECHNICAL REPORT
No.24 (April 1991)

Elastic-Plastic Behavior of Beam-to-Column Connection of High-Strength and Low-Yield Ratio Steel for Building Use

Masamitsu Nagayasu, Hirokazu Yasuda, Shin-ichi Deshimaru, Hiroshi Hujino, Kiyoshi Uchida

Synopsis :
Mechanical properties of the base metal and welded joints as well as low cycle fatigue strength of the beam-to-column connection using low YR (yield ratio) 53 and 60kgf/mm2 steel plates, which have been newly developed for building use, have been investigated. The flexual strength of the beam-to-column connection in full-scale using the materials mentioned above also has been examined. Each steel plate has been demonstrated to be safe and reliable when applied to the steel structure. The principal results obtained are as follows: (1) Steel plates with low YR 53 kgf/mm2 produced by TMCP and 60 kgf/mm2 produced by ferrite and austenite dual-phase region quenching meet aimed properties and have good anti-cracking characteristics. (2) Tensile strength and toughness of the joint are satisfactory, although HAZ softening occurs at welding with a large heat input. (3) Fatigue strength of the beam-to-column connection against the severe earthquake is sufficient. (4) Flexural strength and deformability of the beam-to-column connection with 60 kgf/mm2 steel plates are superior, and improved owing to its low YR.

The body can be viewed from the next page.

Elastic-Plastic Behavior of Beam-to-Column Connection of High-Strength and Low-Yield Ratio Steel for Building Use*


Masamitsu Nagayasu
Senior Researcher, Construction Method Lab., R & D Center, Engineering & Construction Div.


Hirokazu Yasuda
Design & Structures Engineering Sec., Building Engineering Dept., Engineering & Construction Div.

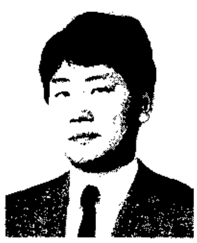
Shin-ichi Deshimaru
Staff Assistant Manager, Plate, Casting & Forging Control Sec., Technical Control Dept., Mizushima Works


Hiroshi Hujino
Staff Manager, Steel Products Technology Dept., Steel Technology Div.


Kiyoshi Uchida
Senior Researcher, Plates, Shapes & Castings Lab., Heavy Steel Products Research Dept., I & S Res. Labs.

Synopsis:

Mechanical properties of the base metal and welded joints as well as low cycle fatigue strength of the beam-to-column connection using low YR (yield ratio) 53 and 60 kgf/mm² steel plates, which have been newly developed for building use, have been investigated. The flexual strength of the beam-to-column connection in full-scale using the materials mentioned above also has been examined. Each steel plate has been demonstrated to be safe and reliable when applied to the steel structure. The principal results obtained are as follows:

(1) Steel plates with low YR 53 kgf/mm² produced by TMCP and 60 kgf/mm² produced by ferrite and austenite dual-phase region quenching meet aimed properties and have good anti-cracking characteristics.

(2) Tensile strength and toughness of the joint are satisfactory, although HAZ softening occurs at welding with a large heat input.

(3) Fatigue strength of the beam-to-column connection against the severe earthquake is sufficient.

(4) Flexual strength and deformability of the beam-to-column connection with 60 kgf/mm² steel plates are superior, and improved owing to its low YR.

1 Introduction

With steel-framed buildings growing larger and taller constructed in increasing numbers, the demand for heavier steel plates of higher tensile strength is expanding. To increase the plastic deformability and seismic energy dissipation capability which are required of steel frames of these high-rise buildings when hit by big earthquakes, steel plates must meet specifications requiring a low yield ratio (YR = yield point/tensile strength) and a low tangent modulus from yield point to strain hardening point ($E_{st'}$). Kawasaki Steel meets these severe specifications by applying the thermomechanical control process (TMCP: or controlled rolling and controlled cooling) for 50- and 53-kgf/mm² steel plates and techniques for heat treatment in the dual phase region for 60-kgf/mm² steel plates. Further, the company has developed low YR steel plates for building use which are excellent in weldability due to their low carbon equivalent (C_{eq}).

The following tests were conducted on 53- and 60-kgf/mm² steel plates, 22 to 100 mm in thickness and produced in an actual commercial line, to verify the soundness of these low YR steel plates for building use, the safety of various kinds of welded joints of these steel plates, the characteristics of structures fabricated from them. Also, the mechanical properties, anti-cracking characteristics, acoustic anisotropy, etc., were investigated for the base metal. For welded joints, joint performance tests by welding with a large heat input (i.e., by the consumable electroslag (CES) welding of

---

* Originally published in *Kawasaki Steel Giho*, 22(1990)1, pp. 29-36

Table 1 Aimed properties of low YR steel plates for building structure use

	Tensile properties*1					Impact value*2		Anisotropy
	YP (kgf/mm²)	TS (kgf/mm²)	YR (%)	El (%)	$E_{st'}$	Test temp. (°C)	Absorbed energy (kgf·m)	Ultrasonic wave velocity ratio (V_L/V_C)
53 kgf/mm² steel	36≦	53~65	≦75	21≦	—	0	2.8≦	0.98~1.02
60 kgf/mm² steel	45≦	60~73	≦80	20≦	≦1/30E	−5	4.8≦	0.98~1.02

*1 T-direction, t/4, JIS Z 2201 4, *2 T-direction, t/4, JIS Z 2202 4

diaphragms used to fabricate square steel pipe columns and submerged-arc welding (SAW) of corner seams), low cycle fatigue tests of beam-to-column connections, full-scale experiments on actual-size models of cruciform beam-to-column connection under antisymmetric loads on beam ends were carried out. This report presents the results of these experiments.

2 Properties of Low YR Steel Plates for Building Use

The targeted properties of the steel plates for building use employed this time are shown in **Table 1**. Maximum values of YR for both the 53- and 60-kgf/mm² steels and of $E_{st'}$ for the 60-kgf/mm² steel are set.

2.1 Manufacturing Processes

The manufacturing process of low YR 53-kgf/mm² steel plates is shown in **Fig. 1**. C_{eq} is set at not more than 0.40% to obtain good weldability and toughness of welded joints, and TMCP is applied by using the MACS (multipurpose accelerated cooling system) to ensure strength in the base metal of the heavy plates at this low C_{eq}. Further, the finish rolling temperature is set at not less than 850°C to obtain a low YR and to eliminate acoustic anisotropy (caused by the rolling texture) which obstructs ultrasonic examination.

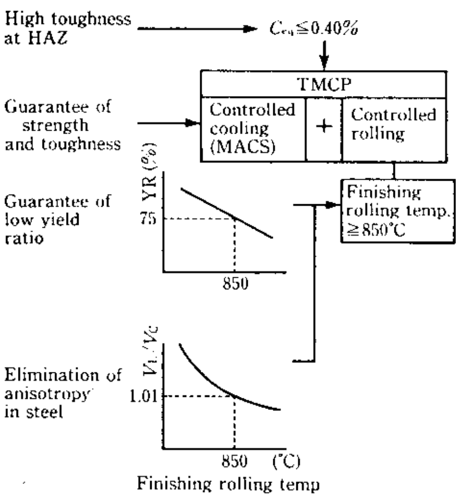

Fig. 1 Technical approach to production of low YR 53 kgf/mm² steel

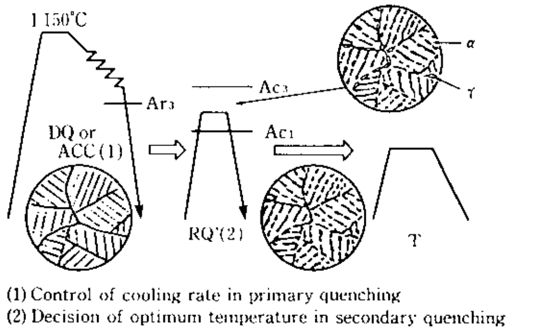

Fig. 2 Changes of microstructure in Q-Q′ process

The manufacturing process of low YR 60-kgf/mm² steel plates is shown in **Fig. 2**. The double quenching process (Q-Q′-T) is applied in which, after plate rolling, primary quenching (Q) is conducted using the ACC (accelerated controlled cooling) or DQ (direct quench) of the MACS equipment and secondary quenching (Q′) is then conducted in the $\alpha + \gamma$ dual-phase region[1,2]. This process is aimed at lowering the YR by generating a texture in which hard layers composed of bainite and martensite and soft layers of ferrite are present.

2.2 Properties of Base Metal

The chemical compositions of the two steels are given in **Table 2**. The REM (rare-earth element)-Ti treatment is conducted to obtain toughness with a large heat input[3]. The resulting of measurements of mechanical properties and acoustic anisotropy are shown in **Table 3**. In both steels, the tensile properties aimed at were quite satisfactory and their impact properties were also good. The acoustic anisotropy was within the targeted levels and seemed to pose no problems.

A Y-groove cracking test was conducted with a heat input of about 20 kJ/cm using SMAW and GMAW. In the low YR 53-kgf/mm² steel plates, the temperature for preventing weld cracking was 20°C in both welding processes. This temperature was 80°C in SMAW with the 60-kgf/mm² steel plates, while it was only 60°C in GMAW.

Table 2 Chemical compostions of low YR steel plates (wt.%)

Steel	C	Si	Mn	P	S	Cu	Ni	Mo	V	Others	C_{eq}*1	P_{cm}*2
53 kgf/mm²	0.13	0.41	1.31	0.005	0.0017	0.15	0.12	0.003	0.003	REM-Ti treat.	0.37	0.22
60 kgf/mm²	0.12	0.27	1.44	0.006	0.0020	0.23	0.19	0.220	0.041	REM-Ti treat.	0.43	0.23

*1 $C_{eq}=C+Si/24+Mn/6+Cr/5+Mo/4+Ni/40+V/14$

*2 $P_{cm}=C+Si/30+(Mn+Cu+Cr)/20+Mo/15+V/10+Ni/60+5B$

Table 3 Mechanical properties and anisotropy of low YR steel plates

Steel	Thickness (mm)	Tensile test*1 YP (kgf/mm²)	TS (kgf/mm²)	YR (%)	El (%)	E_{st}	Impact test $_vE$*2 (kgf·m)	Anisotropy test*3 V_L/V_C	V_L/V_Q
53 kgf/mm²	40	42.6	57.3	74	33	E/53	13.3	1.00	1.00
	60	40.2	54.7	73	35	E/52	17.6	1.00	1.00
	100	39.1	54.8	71	32	E/48	13.4	1.00	1.00
60 kgf/mm²	22	53.0	68.0	78	29	E/40	20.2	1.01	1.00
	40	49.8	63.7	78	31	E/62	21.8	1.01	1.00
	60	47.1	62.7	75	31	E/53	21.4	1.01	1.00
	100	48.0	69.4	69	28	E/35	20.5	1.00	1.00

*1 T-direction, t/4, JIS Z 2201 4, mean of the two test pieces

*2 T-direction, t/4, JIS Z 2202 4, 0°C (53 kgf/mm² steel), −5°C (60 kgf/mm² steel)

*3 Ultrasonic velocity ratio

3 Properties of Welded Joints

3.1 Mechanical Properties

Welded joints were produced using SAW and CES that use a large heat input, and various tests were conducted. The same tests were carried out on cruciform beam-to-column connections welded by GMAW and CES. The welding conditions employed are given in **Table 4**. For SAW, 40- and 60-mm-thick steel plates were welded with a single pass using multiple electrodes and 100-mm-thick steel plates were welded by full-penetration multipass welding with a narrow groove. In the case of CES, the 60-kgf/mm² steel was excluded because it is unnecessary for fabricating diaphragms for stress reasons. Examples of the macrostructure of welded joints are shown in **Photo 1**.

The results of the tensile test of welded joints are shown in **Table 5**. In some CES welded joints produced with a heat input of more than 500 kJ/cm, the joint strength decreased by 1.5 kgf/mm². In other welded joints, however, the feared effect of a large heat input

Table 4 Welding conditions

Welding method	SAW			CES			CES+GMAW	
Groove shape	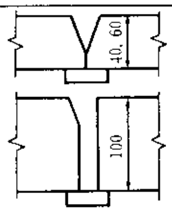			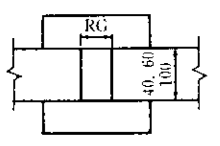 t: 40, 60, 100; RG: 23, 26, 30			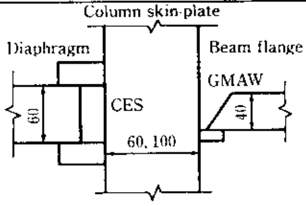	
Steel (kgf/mm²)	53, 60			53			Diaphragm: 53; CS: 53, 60; BF: 53, 60	
Welding materials	Wire: KW30T (53 kgf/mm²) KW101B (60 kgf/mm²) Flux: KB 110 (40, 100 mm^t) KB 501 (60 mm^t)			Wire: KW 50C Flux: KF 100 Consumable nozzle : KU 1 000-10φ			[CES] Same as the left [GMAW] Wire: KC50 (53 kgf/mm²) KC60 (60 kgf/mm²) Shielding gas: CO_2 100%	
							CES	GMAW
Thickness (mm)	40	60	100	40	60	100	60	40
Total passes	1	1	25	1			1	22
Heat input (kJ/cm)	227	436	40×24 222×1	539	851	1721	886	21×22

(a) SAW (60 kgf/mm^2 steel)
(b) CES (53 kgf/mm^2 steel)
(c) CES + GMAW

Photo 1 Macrostructures of welded joints

Table 5 Tensile strength of welded joints

Welding method	Steel (kgf/mm^2)	Thickness (mm)	TS*1 (kgf/mm^2)	Location of fracture
SAW (Butt)	53	40	58.7	HAZ
		60	56.1	WM
		100	56.1	WM-BM
	60	40	65.4	HAZ
		60	65.0	HAZ-BM
		100	68.4	WM
CES (Butt)	53	40	55.8	HAZ
		60	55.3	HAZ
		100	53.8	HAZ
CES +GMAW (Cross)	53	40*2	58.1	BM (BF)
	60	40*2	63.9	BM (BF)

*1 Mean of the two test pieces
TP: W=25 mm, t=Original thickness,
parallel length=100 mm (Butt), 260 mm (Cross)
*2 Plate thickness of beam flange

The face bend test, root bend test and side bend test specified in JIS Z3122 were conducted on SAW and CES welded joints. Relatively large bend defects included a 1.5 mm crack along the columnar crystals of weld metal initiated by the side bending of an SAW welded joint of 53-kgf/mm^2 steel plate of 100 mm thickness, and a 2.8-mm intergranular fracture which occurred in the weld metal structure by the face bending of a CES joint of 60-mm-thick plate. However, both defects were not more than 3 mm. The bending properties seemed not to be effected, considering that an increase in weld heat input scarcely caused cracking.

A Charpy impact test was conducted on SAW joints and cruciform joints by CES and GMAW. The test results are shown in **Tables 7** and **8**. Relatively low toughness values were obtained in the SAW joints of 40- and 60-mm-thick plates and CES cruciform joints (diaphragm of 53-kgf/mm^2 steel, column skin plate in the thickness direction), because all of them were welded in a single pass with a large heat input. However, there seemed to be no special problems because these impact values are higher than the targeted values of the base metals ($_{v}E_0 \geq 2.8$ kgf·m for the 53-kgf/mm^2 steel and $_{v}E_{-5} \geq 4.8$ kgf·m for the 60-kgf/mm^2 steel) and because stresses were structurally small in the corner seam and where the diaphragm was installed by CES.

A Vickers hardness test was conducted on SAW joints of 53- and 60-kgf/mm^2 steel plates, 60 mm in thickness, and CES joints of 53-kgf/mm^2 steel plates, 40 and 100 mm in thickness. In both steels, the softening of the HAZ by welding with a large heat input was observed; in the SAW joints (heat input: 436 kJ/cm) the minimum hardness value was HV (10) ≒ 160 for

Table 7 Charpy impact values of SAW joints

(kgf·m)

Steel (kgf/mm^2)	Thickness (mm)	WM	FL	HAZ	V-notch position
53 ($_{v}E_0$)	40	4.0	5.9	5.3	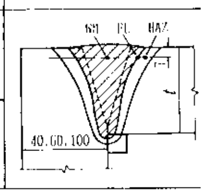
	60	5.6	4.9	5.3	
	100	13.6	16.9	16.9	
60 ($_{v}E_{-5}$)	40	12.8	7.7	6.1	
	60	11.2	5.6	5.0	
	100	18.1	13.1	7.9	

Note: Mean of the three test pieces. TP; JIS Z 2202 4

on the softening of HAZ was scarcely observed in both steels, since HAZ is narrower and slanted, and the same strength as for the base metal (Table 3) was obtained. **Table 6** shows the tensile properties of skin plates of square pipe columns. A skin plate is affected by weld heat in CES for installing a diaphragm and in GMAW for installing a beam flange. The same values of yield point and strength as for the base metal were obtained in all welded joints, with the exception of 60-kgf/mm^2 steel plate of 100 mm thickness which provides high base metal strength.

Table 6 Tensile properties of skin-plate suffered welding heat

Steel	Thickness (mm)	YP (kgf/mm^2)	TS (kgf/mm^2)	El (%)	YR (%)	Test piece
53 kgf/mm^2	60	38.9	54.2	33	72	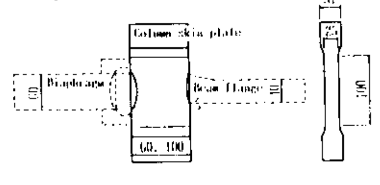
	100	38.7	55.0	49	70	
60 kgf/mm^2	60	48.6	62.4	39	78	
	100	50.3	66.5	35	76	

Table 8 Charpy impact values*1 of cross joints (kgf·m)

Steel (kgf/mm²) CS, BF	Location	Diaphragm*2		Column skin-plate						Beam flange			V-notch position
		HAZ	FL	CES WM	FL	HAZ	t/2	HAZ	FL	GMAW WM	FL	HAZ	
53 (vE_0)	T	4.6	5.0	5.1	4.9	6.2	12.4	22.8	17.8	16.3	16.1	15.9	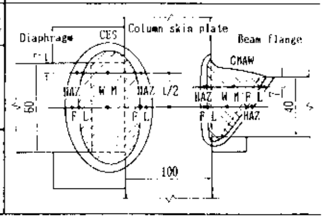
	M	3.3	5.2	4.7	5.7	3.2	13.0	17.2	15.3	12.5	15.5	16.1	
60 (vE_{-5})	T	—	—	6.8	10.8	8.5	9.0	12.7	6.1	6.0	12.6	14.9	
	M	—	—	7.7	11.1	5.0	8.9	23.4	5.5	8.1	9.4	12.7	

*1 Mean of the three test pieces (JIS Z 2202 4) *2 53 kgf/mm² steel

the 53-kgf/mm² steel and HV (10) ≒ 190 for the 60-kgf/mm² steel. In these two cases, the hardness values are about 30 kgf/mm² lower than those of the base metals. Further, in the CES joints of 53-kgf/mm² steel, the minimum value showed HV (10) ≒ 145 for both plate thicknesses of 40 and 100 mm (heat input: 539 and 1721 kJ/cm), indicating that the larger the heat input, the wider the HAZ. However, the above results of the tensile test show that this hardness decrease in the HAZ does not have a great effect on the strength of joints.

From these results, it is apparent that when 53- and 60-kgf/mm² steel plates are welded by SAW and CES with a large heat input, the tensile and bending properties and toughness of welded joints meet the targeted values of the base metals although the welded joints show a decrease in strength and worsening of impact properties.

3.2 Low Cycle Fatigue Characteristics

When a high-rise steel structure is hit by a big earthquake, beam-to-column connections repeatedly undergo compressive and tensile strains in the plastic zone. For this reason, a low-cycle fatigue test was conducted to investigate the yield strength of the low YR steel using the specimen shown in **Fig. 3**, which is a model of a connection between a square steel pipe column and an H-beam. Three kinds of specimen were used by fabricating both the column and the beam from 53- or 60-kgf/mm² steel; the column from 60-kgf/mm² steel and the beam from 53-kgf/mm² steel. The plate thickness was 40 mm for the beam and 100 mm for the column. A 53-kgf/mm² steel of 60-mm thickness was used for the diaphragm. The diaphragm was welded to the column by CES using water-cooled copper straps, and the beam was welded to the column by GMAW (for the welding conditions, refer to Table 4). Tensile and compressive strains of 1 to 4% were applied while being controlled using a strain gauge (WSG) put to the parallel part of the beam (base metal portion).

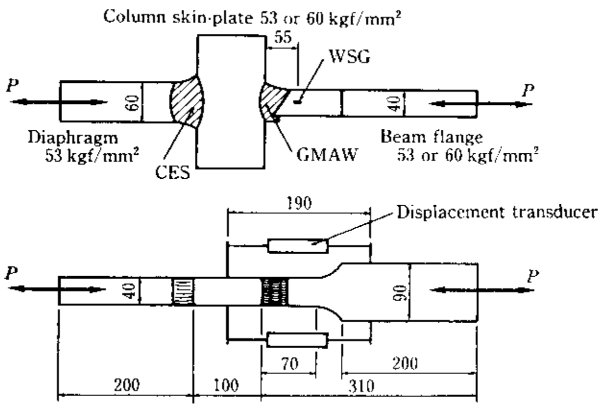

Fig. 3 Fatigue test specimen

The results of the fatigue test are summarized in **Table 9**, and examples of hysteresis of load-strain relation are shown in **Fig. 4**. In each specimen, the stress at the point of inversion increases during the second cycle but remains steady after that; in this steady state the beam of 53-kgf/mm² steel showed a slight tendency toward work hardening, and the beam of 60-kgf/mm² steel toward work softening. In all the specimens, a crack was initiated in the back bond of the weld (GMAW) at the beam and this crack propagated along the weld zone as if joining with another crack produced in the surface bond, resulting in failure. An example of the failure is shown in **Photo 2**. This fracture condition is different from the break in the base metal of the beam which occurred in the static cross tension described in the preceding paragraph. **Figure 5** shows the relationship between strain amplitude and number of cycles to failure in the 53- and 60-kgf/mm² steel used in the beams which fractured. The number of cycles is larger in the 60-kgf/mm² steel than in the 53-kgf/mm² steel; this tendency is different from the results of a past study which indicated that the higher the tensile strength of steel, the shorter the fatigue life.[4)]

Usually, when a steel structure is hit by a big earthquake, the number of cycles of the strain which exceeds the yield stress at the beam-to-column connections is at most ten,[5)] and the strain amplitude is considered not to exceed ±3% at most, according to a study by Mukudai et al.[6)]. It can be estimated from **Fig. 5** that both the 53- and 60-kgf/mm² steel in question can withstand strain amplitudes of up to ±3.5% (17.5 times the yield

Table 9 Low cycle fatigue test results of cross joints

Test piece	Steel (kgf/mm²) DF-CS-BF	Strain amplitude (%)	σ_t/σ_y	σ_c/σ_y	N_f (cycle)
A-2	53-53-53	±2	1.32	−1.45	34
A-4		±4	1.43	−1.62	7
B-1	53-60-53	±1	1.17	−1.22	74
B-2		±2	1.29	−1.39	21
B-3		±3	1.46	−1.61	14
B-4		±4	1.53	−1.70	9
C-1	53-60-60	±1	1.04	−1.10	150
C-2-1		±2	1.20	−1.32	41
C-2-2		±2	1.19	−1.28	44

Note (1) σ_y: Yield stress at first loading cycle (3) N_c: Number of cycles to crack
(2) $\sigma_{t,c}$: Stress at stable hysterisis loop (4) N_f: Number of cycles to failure

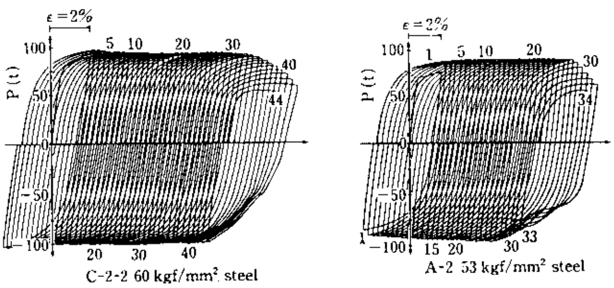

Fig. 4 Load-strain hysteresis loop

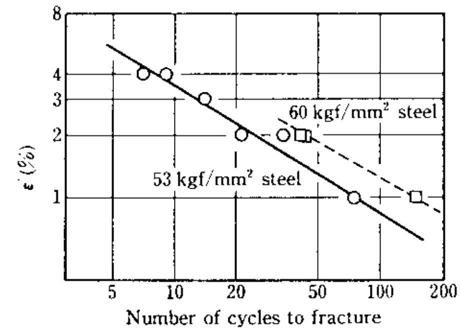

Fig. 5 Relation between strain and number of cycles to fracture

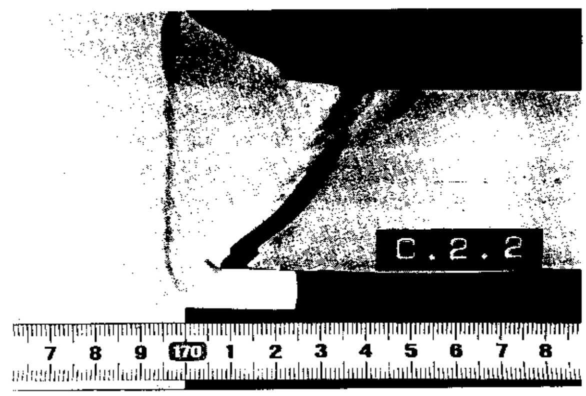

Photo 2 Appearance of fractured low cycle fatigue test specimen (strain amplitude = ±2%)

stress if it is 0.2%) for ten cycles. Therefore, it may be said that the beam-to-column connections of the two steels have sufficient low-cycle fatigue strength.

4 Flexural Strength and Deformability of Actual-Size Beam-to-Column Connection

A beam-to-column connection is structurally the most important part and the various behaviors of structures are directly influenced not only by the properties of steel, but also by the welded joint performance of connections. To investigate the safety of beam-to-column connections of low-YR 60-kgf/mm² steel plates, therefore, an actual-size specimen was produced and a loading test was conducted and the plates strength and deformability were examined.

4.1 Specimen and Methods of Experiment

The specimen used is shown in **Fig. 6**. This is a cruciform frame of a beam-to-column connection, 4 m in story height and 8 m in span, assumed to be used in the lower stories of a high-rise buildings. The square column 600 mm x 600 mm x 60 mm was assembled by one-pass SAW with full penetration of corner seams (Photo 1), and the H-beam 800 mm x 300 mm x 22 mm x 40 mm was assembled by SAW with partial penetration (leg length: 14 mm). They were made of the low-YR 60 -kgf/mm² steel plates shown in Table 3. Incidentally, a diaphragm of 40-mm-thick plate of 53-kgf/mm² steel was installed in the square steel pipe column. To connect the beam to the column, full-penetration SMAW was conducted using a double-bevel

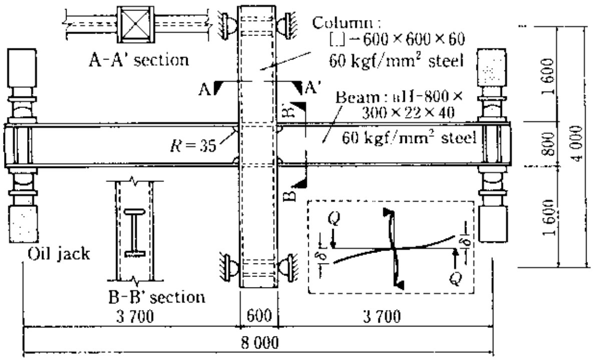

Fig. 6 Bending test specimen and loading condition of beam to column connection

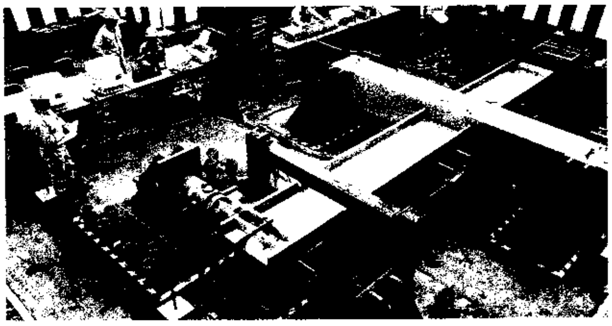

Photo 3 Overview of full-scale flexural test

groove by installing a scallop on the beam web and an end tab on the end of the beam flange. Assuming the loading during an earthquake to be the bending due to antisymmetric load Q on the beam end, axial force on the column was not introduced. The overall deformation δ of the beam end and the shearing deformation of the panel zone were measured with a displacement meter, and the strain of principal parts that enter the plastic zone, such as beam connections, were measured with applied strain gauges WSG. In the experiment, unidirectional loading to induce a fracture was conducted after repeated application of increasing cyclic loads (8 cycles) to three times the deformation of the beam at the yield strength (${}_aQ_y$: calculated value). How the experiment was conducted is shown in **Photo 3**.

4.2 Results of Experiment

The relationship between applied load on the beam end and overall deformation of the specimen (Fig. 6) is shown in **Fig. 7** and the fracture condition of the specimen is shown in **Photo 4**. Microcracks initiated in the toe of the weld of the tension flange of the beam and propagated, and simultaneously local buckling and out-of-plane deformation occurred in the compression flange and the beam showed a maximum strength ${}_eQ_m$ of 223 t. After that, the tension flange was broken. The ultimate strength ${}_eQ_u$ was 222 t, which was not low when compared to the maximum strength. During the experiment, there was no abnormal change in the

(a) Compression flange (b) Tension flange

Photo 4 Failure of test specimen

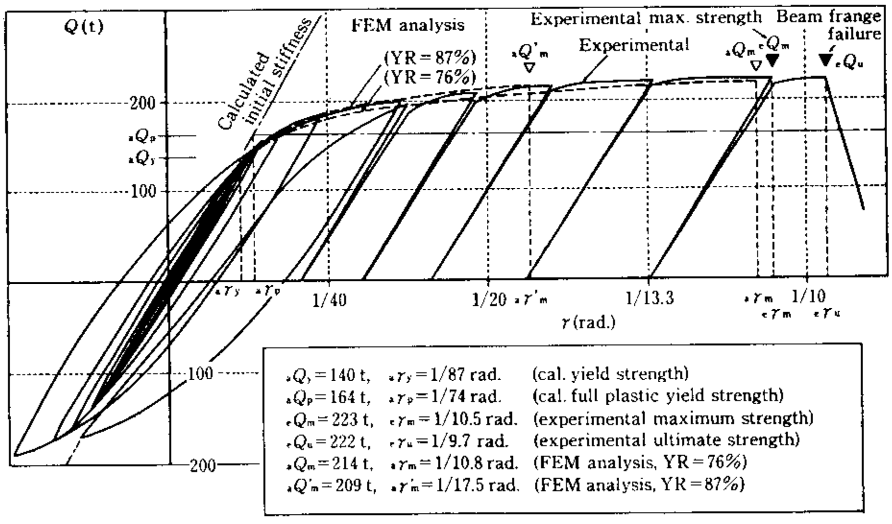

Fig. 7 Load-deformation curves by the experiment and FEM analysis

column or panel zone. After the experiment, a macroetching test of the specimens' corner seam and welds for installing the diaphragm was conducted and no damage, such as cracks, were found.

4.3 Maximum Strength and Deformability

The maximum strength tends to decrease since the stress shared by the beam web of the H-shape decreases due to the out-of-plane bending of the skin plate of the square pipe column, because the beam section decreases due to the scallop installed in the beam web, thus concentrating strain on the beam flange. However, the maximum strength obtained in this experiment, ${}_{e}Q_{m} = 223$ t, is 1.36 times the full plastic yield strength of the beam ${}_{a}Q_{p} = 164$ t (calculated value) and is considered to be high. Compared with the past examples of experiments on 60 kgf/mm^2 of relatively high YR[7], the maximum strength of the present steel is satisfactory.

The overall deformation angle at the maximum strength is 1/10.5 rad., which is 8.29 times the value obtained at the yield strength of the beam. Therefore, the deformability of the present steel is good. This is because the plastic deformability of a beam having a moment gradient is governed by the length of the plastic zone generated at the beam end. This can be understood from the fact that the plastic zone of the beam flange expands up to more than 1 000 mm owing to the use of the present low-YR steel, as is apparent from the results of strain measurement shown in **Fig. 8**.

To confirm these points, an elastic-plastic analysis of this specimen was made using 76% and 87% for YR. In this analysis, the specimen was modeled using heavy-wall shell elements (1/2 model with the beam web serving as the plane of symmetry) and was approximated by five polygonal lines to the stress-strain curve of the steel up to the maximum stress intensity to examine the elastic-plastic behavior under increasing monotonic loads. The results of the analysis are shown in Fig. 7. The plastic zone at the maximum strength was estimated by applying the yield conditions of von Mises (**Fig. 9**). The results of the analysis reveal that at a YR of 76%, there is a good correspondence between the results of the analysis and those of the experiment; the difference is only 4% in terms of the maximum strength and within 3% in terms of the overall deformation angle under this strength. It was also revealed that the increase in flexural strength after the yield of the

Fig. 8 Strain distribution in beam end (longitudinal)

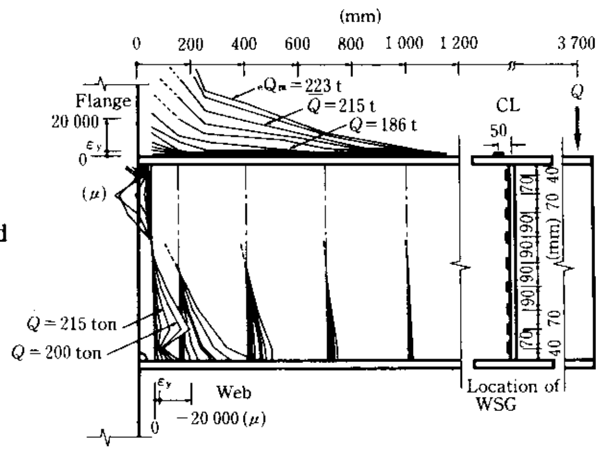

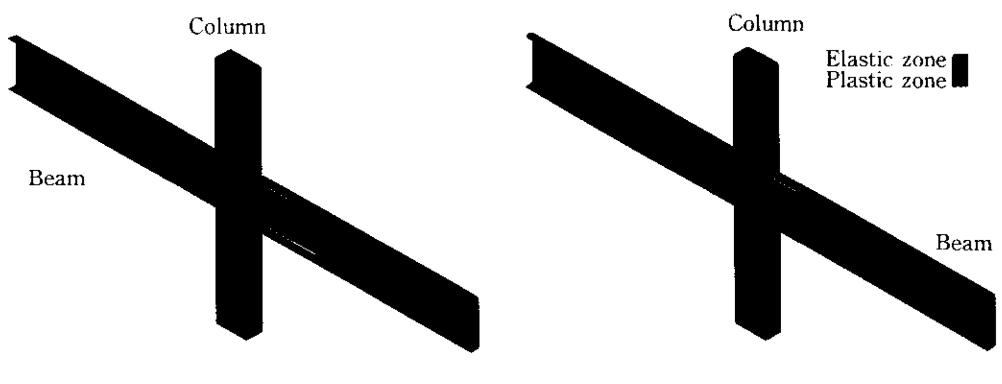

(a) Low YR steel (YR = 76%) (b) High YR steel (YR = 87%)

Fig. 9 Von Mises stress distribution at maximum strength of beam, FEM analysis result specimen is larger in the low YR steel than in the high YR steel and that deformability improves substantially due to the expansion of the plastic zone of the beam.

From the above, it may be said that beam-to-column connections of low-YR 60-kgf/mm^2 steel plates have sufficient deformability and good antiseismic performance.

5 Conclusions

Various performance tests were conducted on low-YR 53- and 60-kgf/mm^2 steel plates produced in an actual line and the following results were obtained:

(1) Tests for Mechanical Properties of Base Metal:

(a) Low-YR 53-kgf/mm^2 steel plates produced by the TMCP and 60-kgf/mm^2 steel plates quenched in the dual-phase region produce the targeted tensile properties (YR, E_{st}, etc.), toughness, etc. and show little acoustic anisotropy.

(b) The 53-kgf/mm^2 steel plates have good weld cracking resistance according to the Y-groove cracking test, and it is unnecessary to conduct preheating if the base metal temperature is not less than 20°C. In the 60-kgf/mm^2 steel plates, the temperature for preventing weld cracking is 80°C for SMAW and this temperature can be lowered by 20°C by using GMAW.

(2) Performance Test of Welded Joints:

(a) In both steel grades, the heat-affected zone softens in welded joints produced with a large heat input. However, the strength of the joints scarcely decreases and the same strength as that of the base metal was obtained.

(b) The toughness of welded joints produced with a large heat input decreases in the bond and HAZ. However, the same strength as that of the base metal can be assured.

(c) There is no problem in the bending properties of joints.

(3) Low Cycle Fatigue Test of Beam-to-Column Connections:

(a) The low-cycle fatigue strength of beam-to-column connections of 60-kgf/mm^2 steel plates is equal to or higher than that of 53-kgf/mm^2 steel plates.

(b) Failure occurs when a crack initiated in the bond of a weld propagates. The mechanism of this failure is different from that of the break of the base metal under static tension.

(c) There is no practical problem in the fatigue strength of the two steel grades.

(4) Experiment on Actual-Size Beam-to-Column Connections:

(a) Actual-size beam-to-column connections of low-YR 60-kgf/mm^2 steel plates showed maximum strength accompanied by buckling at the compression flange of the beam. After that, the tension flange was ruptured at the weld zone where the beam was connected to the column.

(b) The maximum strength is sufficient marking 1.36 times the full plastic yield strength.

(c) The overall deformation angle at the maximum strength is 1/10.5 rad., which is 8.29 times the value upon the yield of the beam and is sufficient.

(d) the experimental values of maximum strength and overall deformation angle are in good agreement with the analytical values of FEM.

(e) The maximum strength and deformability of steel are improved by lowering its YR.

From the above, it was found that the properties of the base metal and welded joints of low-YR 53- and 60-kgf/mm^2 steel plates for building use are good and that their structural performance is also excellent.

The authors would like to extend their sincere thanks to Professor Koji Morita, Chiba University, for his guidance and Professor Koich Takanashi, Tokyo University, for his helpful advice in carrying out these experiments.

References

1) K. Uchida, Y. Kataoka, Y. Oka, and S. Deshimaru: *CAMP-ISIJ*, **2**(1989)3, 874

2) S. Deshimaru, E. Kobayashi, K. Uchida, S. Ueda, M. Nagayasu, and H. Fujino: *CAMP-ISIJ*, **2**(1989)3, 875

3) S. Deshimaru, I. Hirai, K. Amano, S. Ueda, T. Uemura, and K. Tsubota: "Production of Heavy-Gauge Steel Plates Suitable for High-Heat Input Welding in the Arctic Region", *Kawasaki Steel Giho*, **18**(1986)4, 301

4) K. Kaneta, and I. Kohzu: "Low-Cycle Fatigue Strength of Welded Steel Structural Joints Part 1, Low-cycle fatigue of cylindrical specimens using mild to high tensile strength steels", Transactions of the Architectural Institute of Japan, 313(1982), 30–38

5) Study Group "SAWED": "Defect Estimation and Safety of Steel Structures Part 6. Assessment Method for Flaws in Weld Connections of Building Frame", JSSC, **12**(1976)124, 27–33

6) Y. Mukudai, Y. Matsui, and A. Matsuo: "A Study on Deformation Capacity and Low Cycle Fatigue Characteristics of a Defective Welding Joint", *Journal of Structural Engineering (Architectural Institute of Japan)*, **34B**(1988), 131–140

7) C. Matsui, K. Tsuda, T. Ukishima, and J. Sakai: "Studies on the Development of SRC Structures Using High-Strength Steel No. 29, Tests of SRC and Steel Cruciform Frames (Part 1) Test Program and Results of Steel Frames", Summaries of Technical Papers of Annual Meeting (Architectural Institute of Japan), Structures II, (1987), 1259–1260